Journal of the Iranian Chemical Society
https://doi.org/10.1007/s13738-021-02156-5

ORIGINAL PAPER

Synthesis, characterization, in vitro biological and computational evaluation of 5-benzyl-4-(benzylideneamino)-2*H*-1,2,4-triazole-3(4*H*)-thiones

Hamid Aziz[1] · Aamer Saeed[1] · Ashfaq Ur Rehman[2,3] · Farukh Jabeen[4,5] · Bakht Nasir[6] · Ashraf Ullah Khan[6] · Ismat Ullah Khan[7]

Received: 8 June 2020 / Accepted: 2 January 2021

Abstract

Triazoles and their heterocyclic analogues are nitrogen-rich versatile pharmacophores easily synthesized and converted to a range of biologically relevant heterocycles. In this context, the present research reports the synthesis, characterization, in vitro antioxidant, cytotoxic and α-glucosidase inhibitory potential of 4-amino-5-benzyl-2*H*-1,2,4-triazol-3(4*H*)-thione **(3)** and 5-benzyl-4-(benzylideneamino)-2*H*-1,2,4-triazole-3(4*H*)-thiones **5(a–g)**. Consequently, the percent DPPH free radical scavenging ability was found to be in the decreasing order of **5 g > 5e > 3 > 5d > 5b > 5c > 5a > 5f**. The most potent derivatives **(5 g), (5e)** and **(3)** showed significant dose-dependent scavenging ability with IC_{50} values of 61.22, 74.06 and 94.87 µg/ml, respectively. The antioxidant derivatives were screened in brine shrimp lethality as well as protein kinase inhibitory assay to unveil their toxic nature. The percent mortality was found to be decreasing in the order of **5b > 5f > 3 > 5a > 5 g > 5 d > 5e > 5c** at 200 µg/ml in brine shrimp lethality assay. Accordingly, three derivatives **(5b)**, **(3)** and **(5f)** showed significant percent mortality with LC_{50} values of 25.88, 32.94 and 34.87 µg/ml, respectively. Similarly, in protein kinase inhibitory assay, maximum inhibitory potential was observed for the derivatives **(5 g)**, **(3)** and **(5e)** with MIC values of 50 µg/disc in each case. Likewise, in α-glucosidase inhibition assay, the screened derivatives **(3)** and **(5e)** showed notable percent α-glucosidase inhibition (66.78 and 55.15%) with IC_{50} value of 36.11 µg/ml and 60.33 µg/ml, respectively. Molecular docking studies of the screened derivatives were performed in order to assess their binding potential and mechanism of their binding with α-glucosidase, α-kinase and β-kinase enzymes. Docking simulation revealed that the molecules stabilize themselves inside

✉ Aamer Saeed
aamersaeed@yahoo.com

1 Department of Chemistry, Quaid-I-Azam University Islamabad, Islamabad 45320, Pakistan

2 Department of Biochemistry, Abdul Wali Khan University, Mardan, Shankar Campus, Mardan 23200, Khyber Pukhtoonkhwa, Pakistan

3 Department of Bioinformatics and Biostatistics, Shanghai Jiao Tong University, 800 Dongchuan Road, Minhang District, Shanghai 200240, People's Republic of China

4 Department of Chemistry and Biochemistry, Laurentian University, 935 Ramsey Lake Road, Sudbury, ON P3E 2C6, Canada

5 Computation, Science, Research and Development Organization, 1401, 2485 Hurontraio Street, Mississauga, ON L5A2G6, Canada

6 Department of Pharmacy, Quaid-I-Azam University Islamabad, Islamabad 45320, Pakistan

7 Institute of Chemical Sciences, Gomal University, Dera Ismail Khan 29220, Khyber Pukhtoonkhwa, Pakistan

Published online: 26 January 2021

the active site by establishing non-covalent interactions with critical residues. Noteworthy were the derivatives (**3**) and (**5e**) which anchored themselves through various significant electrostatic interactions with the critical residues.

Graphic abstract

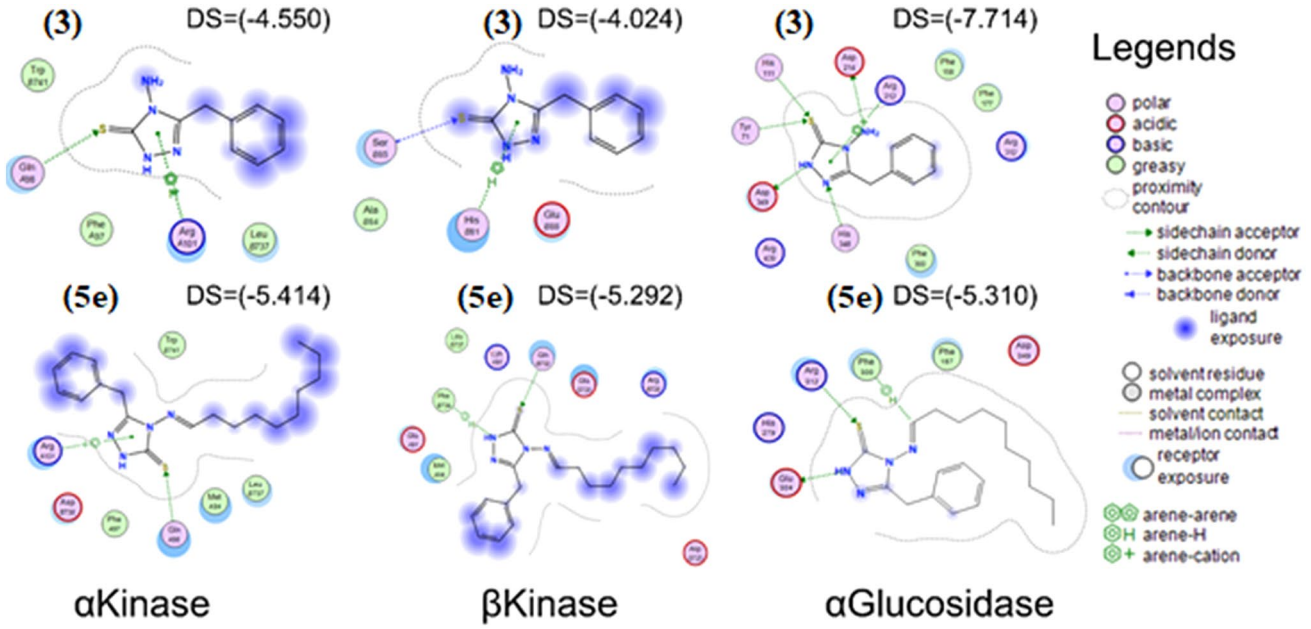

Keywords Antioxidants · DPPH · Molecular docking · Protein kinase inhibitors · Triazoles

Introduction

1,2,4-Triazoles are nitrogen-rich five-membered aromatic heterocycles with molecular formula $C_2H_3N_3$, commonly known as bio-isostere of oxadiazoles [1]. Depending on the relative positions of N-atoms in the ring, triazoles occur in two isomeric forms: 1,2,4-triazoles or 1,2,3-triazoles. Both these isomers of triazoles show tautomerism and are found in two forms, i.e., 1,2,4-triazoles can occur as 1,2,4-(4*H*)-triazoles and 1,2,4-(1*H*)- triazoles, whereas 1,2,3-triazoles can occur as 1,2,3-(2*H*)-triazole and 1,2,3-(1*H*)-triazole. 1,2,4-triazole moiety has gained considerable attention of scientists due to its vast range of uses in pharmaceuticals, material sciences, and agrochemicals [2]. For example, variously substituted 1,2,4-triazoles are described to have vast range of biological activities like antimicrobial, antifungal [3], anti-inflammatory [4], antibacterial [5], hypoglycemic [6], anti-tubercular [7], antidiabetic [8], anticonvulsant [9], antidepressant [10], anti-malarial [11], anti-migraine [12], analgesic [13], arthritis [14], antiviral [15], antihypertensive [16, 17], antileishmanial [18], antiplatelet [19] potassium channel activators [20], and antioxidant [21]. Several 1,2,4-triazoles are commercialized as imperative herbicides, fungicides [22] and growth regulators in plants [23]. 1,2,4-Triazoles possess unusual properties like strong hydrogen bond donor or accepter, moderate dipole character, rigidity and stability which enhances their biological profile [24–26]. The 1,2,4-triazole core shows considerable tolerance to metabolic degradation and exhibits target specificity and vast range of activities. The triazole core due to its polar nature can enhance the solubility of ligands and afford improved pharmacodynamic and pharmacokinetic activities [27]. Moreover, the presence of nitrogen atoms in a triazole ring aids intercalation and impart chromophore a polarized character resulting in an optimal DNA interaction [27–30]. Notable examples include fluconazole, voriconazole and posaconazole used as antimycotic, anti-anxiety and CNS stimulants [31]. 1,2,4-Triazole-based drugs like vorozole, letrozole and anastrozole serve as potent aromatase inhibitors which prevent breast cancer [32]. Thus, 1,2,4-triazole rings are inserted in a range of diverse and therapeutically relevant heterocycles to turn them into efficient drug candidates. Based on the sale values, the 1,2,4-triazole-containing antifungal drugs have made their position in the list of top 200 drugs [33, 34]. The antifungal drugs with 1,2,4-triazole core include voriconazole, ravuconazole and itraconazole [35, 36]. Consequently, some of the potent and commercially available 1,2,4-triazole-based drugs are shown in Fig. 1.

Schiff bases are nitrogen analogues of aldehyde and ketones containing imine/azomethine linkage in their

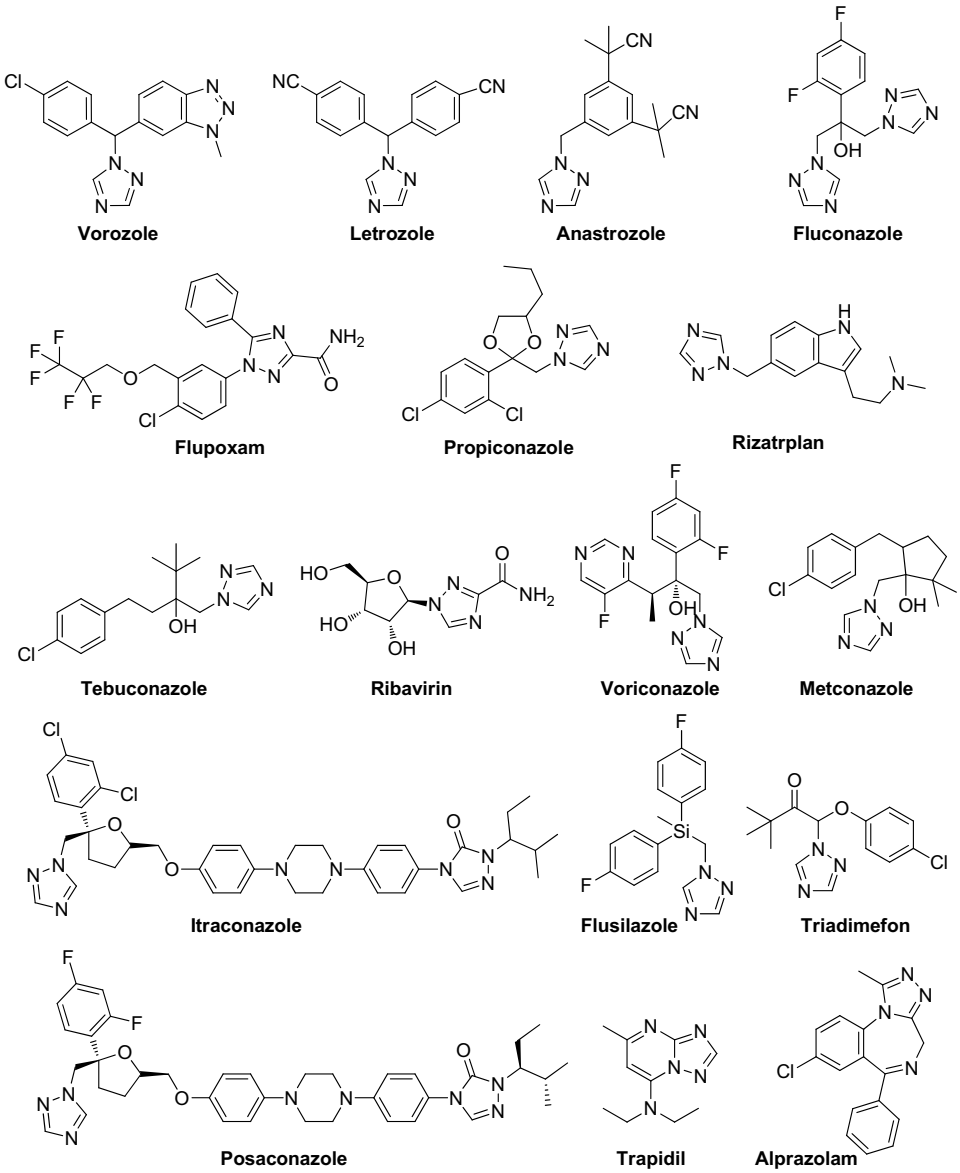

Fig. 1 Some commercially available drugs containing 1,2,4-triazole core skeleton

structures [37] and are frequently utilized for industrial means and exhibit diverse biological activities [38]. They are found in various natural, natural-derived and non-natural heterocycles [39–41]. Their electrophilic carbon and nucleophilic nitrogen atoms interact nucleophiles and electrophiles that lead to enzymes inhibition and DNA replication [42]. Azomethine linkages impart heterocycles potent biological potential including anticancer, antimicrobial, antipyretic, antiproliferative and antidiabetic [43]. Metal complexes of Schiff bases are very active catalysts in many biological systems [44–47], dyes [48], polymers [49] and medicinal industries [50]. Their uses in food packages, birth control and as an oxygen sensor are also delineated. In this regard, literature survey reveals that the pharmacokinetic profile of 1,2,4-triazoles is improved by incorporating Schiff bases in their core skeleton [51]. 1,2,4-Triazoles-derived Schiff bases are reported as potent and effective antimicrobials [52, 53], antitumor [54], cytotoxic, growth regulating, antioxidant, and antidiabetic agents [55]. Pillai et al. recently reported the enhanced pharmacokinetic profile of novel 4-amino-1,2,4-triazole-based Schiff bases. Based upon the drug-likeness calculations and in vitro antidiabetic assay against α-glucosidase, the screened 4-amino-1,2,4-triazole-based Schiff bases displayed significant inhibitory potential in terms of their IC_{50} values compared to the reference standard acarbose [56]. Moreover, the 4-amino-1,2,4-triazole-based Schiff bases displayed strong antioxidant potential in DPPH and total reducing power assays [56].

Keeping in view the synthetic utility and biological potential of 1,2,4-triazoles, on the one hand, and the enhancement of pharmaceutical potential of the Schiff bases, on the other hand, the current research aims at the

synthesis, characterization, biological evaluation and molecular docking studies of 4-amino-5-benzyl-2*H*-1,2,4-triazole-3(4*H*)-thione and their corresponding 5-benzyl-4-(benzylideneamino)-2*H*-1,2,4-triazole-3(4*H*)-thiones. The synthesis of 4-amino-5-benzyl-2*H*-1,2,4-triazol-3(4*H*)-one was performed in a facile way using thiocarbohydrazide and phenylacetic acid. Condensing 4-amino-5-benzyl-2*H*-1,2,4-triazol-3(4*H*)-one with various aldehydes results in a series of 5-benzyl-4-(benzylideneamino)-2*H*-1,2,4-triazole-3(4*H*)-thiones. The synthesized compounds were identified and confirmed using various spectroscopic techniques like FT-IR, ^{1}H-NMR, ^{13}C-NMR and elemental analysis (CHNS) and were screened in various in vitro biological assays.

Experimental protocols

Chemistry

The reactions were carried out under nitrogen atmosphere using freshly dried distilled solvents obtained from sigma-Aldrich. NMR spectra were recorded using Bruker 300 MHz spectrometer at ambient temperature. The chemical shifts values are reported relative to the residual solvent peak of DMSO (δ 2.50 for ^{1}H and δ 39.52 for ^{13}C) or acetone (δ 2.05 for ^{1}H and δ 29.84, δ 206.26 for ^{13}C). TMS was used as an internal reference, and the ^{1}HNMR data are reported as the chemical shift value (δ), relative integral, multiplicity s (singlet), d (doublet), t (triplet), quartet (q), m (multiplets), b (broad), coupling constant (*J*, Hz), and the atom assignment. ^{13}C NMR data are reported as the chemical shift value (δ) and assignment of the atom. The FT-IR spectra were measured in wave numbers (cm^{-1}) using Vertex 70 Bruker apparatus. Elemental analysis (CHNS) was performed to find out the percentage of each element present in the synthesized compound. Thin layer chromatography (TLC) on 2.0 cm × 5.0 cm aluminum sheets precoated with silica gel 60F254 with a layer thickness of 0.25 mm (Merck) was performed to check the reaction's progress. Ultraviolet fluorescence was used for the identification of the compounds while using TLC.

Synthesis of 4-amino-5-benzyl-2*H*-1,2,4-triazole-3(4*H*)-thione (3)

The 4-amino-5-benzyl-2*H*-1,2,4-triazole-3(4*H*)-thione (**3**) was synthesized efficiently using a reported methodology but with slight modifications. Briefly, equimolar ratios (10 mmol) of phenyl acetic acid and thiocarbohydrazide were mixed in a 100-ml round-bottom flask. The reaction mixture was allowed to stir at room temperature for half an hour (hr) to ensure homogenous mixing of the reactants. After half an hour, the temperature of the reaction mixture was raised up to 90 ℃ for another half an hour. During the course of the reaction, TLC was employed to check the reaction's progress using chloroform/methanol (70:30) solvent system. Once the reaction was completed, the reaction mixture was poured in ice cold water which resulted in the formation of solid precipitates. The resulting precipitates were filtered and dried in an oven at 70 ℃ for two hrs to obtain solid white precipitates of the product [56].

4-Amino-5-benzyl-2*H*-1,2,4-triazole-3(4*H*)-thione (3)

White powder; (80%); R_f; 0.54 (chloroform/methanol, 70:30); m.p 155 ℃; Mol. wt: 206.27; IR (neat, cm^{-1}) ν: 3286.44, 3237.35 (NH_2), 3148.91 (NH), 3084.74, 3033.33 (sp^2 CH), 2934.46 (sp^3 CH), 1624.52 (C=N), 1567.18, 1494.95, 1451.50 (Ar–C=C), 1417.83 (C–N), 1364.01 (-CH bending), 1295.68 (C=S); ^{1}H NMR (DMSO-d_6, 300 MHz) δ: 13.54 (b, s, 1H, NH), 7.33 (d, 2H, J = 6.90 Hz, Ar–H), 7.30 (t, 2H, J = 7.50 Hz, Ar–H), 7.25 (t, 1H, J = 7.50 Hz, Ar–H), 5.55 (s, 2H, C–H), 4.02 (b, s, 2H, NH_2); ^{13}C NMR (DMSO-d_6, 75 MHz) δ: 166.47 (C=S), 151.83 (C=N), 135.96 (Ar), 129.31 (Ar), 128.94 (Ar), 127.25 (Ar), 30.61 (C–H); Anal. Cald. For $C_9H_{10}N_4S$: C, 52.41; H, 4.89; N, 27.16; S, 15.55: Found: C, 52.37; H, 4.94; N, 27.20; S, 15.50.

Synthesis of 5-benzyl-4-(benzylideneamino)-2*H*-1,2,4-triazole-3(4*H*)-thione 5(a–g)

The synthesis of 5-benzyl-4-(benzylideneamino)-2*H*-1,2,4-triazole-3(4*H*)-thiones **5(a–g)** was performed as reported in the literature. Briefly, aldehydes (15 mmol) completely dissolved in (05 ml) dry distilled ethanol containing catalytic amount of concentrated sulfuric acid was stirred at reflux for half an hour. After half an hour, a solution of 4-amino-5-benzyl-2*H*-1,2,4-triazole-3(4*H*)-thione (10 mmol) prepared using dry distilled ethanol (10 ml) was sequentially added to the acidic solution of aldehydes in ethanol. The resulting reaction mixture was set for further 24 h at reflux. During the course of the reaction, TLC was employed to check the reaction's progress using chloroform/methanol (70:30) solvent system. Once the reaction was completed, ethanol was removed under reduced pressure to obtain the product in a solid form which was recrystallized from ethanol at room temperature [56].

5-Benzyl-4-(propylideneamino)-2*H*-1,2,4-triazole-3(4*H*)-thione (5a)

Brown powder; (70%); R_f; 0.50 (chloroform/methanol, 70:30); m.p 165 ℃; Mol. wt: 246.33; IR (neat, cm^{-1}) ν: 3193.62 (NH), 3065.25 (sp^2 CH), 2992.59, 2890.46 (sp^3 CH), 1639.61 (HC=N), 1590.32, 1579.48, 1524.10 (Ar–C=C), 1439.57 (–CH bending), 1371.30 (-CH bending), 1280.52 (C=S); ^{1}H

NMR (CD_3COCD_3-d_6, 300 MHz) δ: 11.28 (b, s, 1H, NH), 7.53 (s, 1H, HC=N), 7.17 (t, 2H, J = 8.10 Hz, Ar–H), 7.10 (t, 1H, J = 8.10 Hz, Ar–H), 7.09 (d, 2H, J = 8.10 Hz, Ar–H), 4.35 (s, 2H, C–H), 1.43 (q, 2H, J = 7.20 Hz, C–H), 0.93 (t, 3H, J = 7.20 Hz, C–H); ^{13}C NMR (CD_3COCD_3-d_6, 75 MHz) δ: 168.0 (C=S), 161.0 (C=N), 156.24 (HC=N), 137.53 (Ar), 129.13 (Ar), 128.73 (Ar), 125.83 (Ar), 30.92 (C–H), 21.83 (C–H), 10.43 (C–H); Anal. Cald. For $C_{12}H_{14}N_4S$: C, 58.51; H, 5.73; N, 22.74; S, 13.02: Found: C, 58.43; H, 5.75; N, 22.70; S, 13.72.

4-(4-Chlorobenzylideneamino)-5-benzyl-2*H*-1,2,4-triazol-3(4*H*)-thione (5b)

Yellow powder; (75%); R_f; 0.45 (chloroform/methanol, 70:30); m.p 212 ℃; Mol. wt: 328.82; IR (neat, cm^{-1}) ν: 3237.70 (NH), 3084.76, 3032.18 (sp^2 CH), 2933.95 (sp^3 CH), 1624.70 (HC=N), 1566.86, 1493.37, 1417.81 (Ar–C=C), 1453.16 (-CH bending), 1360.63 (-CH bending), 1294.05 (C=S); ^{1}H NMR (CD_3COCD_3-d_6, 300 MHz) δ: 11.28 (b, s, 1H, NH), 8.13 (s, 1H, HC=N), 7.65 (d, 2H, J = 8.10 Hz, Ar–H), 7.35 (d, 2H, J = 8.10 Hz, Ar–H), 7.17 (t, 2H, J = 8.0 Hz, Ar–H), 7.09 (t, 1H, J = 8.0 Hz, Ar–H), 7.03 (d, 2H, J = 8.10 Hz, Ar–H), 4.26 (s, 2H, C–H); ^{13}C NMR (CD_3COCD_3-d_6, 75 MHz) δ: 156.62 (C=S), 151.70 (C=N), 149.80 (HC=N), 138.98 (Ar), 135.54 (Ar), 129.43 (Ar), 128.98 (Ar), 128.59 (Ar), 126.98 (Ar), 124.10 (Ar), 30.53 (C–H); Anal. Cald. For $C_{16}H_{13}ClN_4S$: C, 58.44; H, 3.98; N, 17.04; S, 9.75: Found: C, 58.30; H, 3.92; N, 17.14; S, 9.79.

4-(4-Nitrobenzylideneamino)-5-benzyl-2*H*-1,2,4-triazole-3(4*H*)-thione (5c)

Yellow powder; (86%); R_f; 0.32 (chloroform/methanol, 70:30); m.p 135 ℃; Mol. wt: 339.37; IR (neat, cm^{-1}) ν: 3383.39 (NH), 3091.16, 3050.63 (sp^2 CH), 2941.86 (sp^3 CH), 1651.33 (HC=N), 1597.31, 1574.28, 1514.57, 1455.67 (Ar–C=C), 1344.37 (-CH bending), 1266.70 (-CH bending), 1216.20 (C=S); ^{1}H NMR (CD_3COCD_3-d_6, 300 MHz) δ: 12.80 (b, s, 1H, NH), 10.81 (s, 1H, HC=N), 8.40 (d, 2H, J = 8.70 Hz, Ar–H), 8.19 (d, 2H, J = 9.0 Hz, Ar–H), 7.40 (d, 2H, J = 7.2 Hz, Ar–H), 7.32 (t, 2H, J = 7.50 Hz, Ar–H) 7.25 (t, 1H, J = 7.20 Hz, Ar–H), 4.29 (s, 2H, C–H); ^{13}C NMR (CD_3COCD_3-d_6, 75 MHz) δ: 156.64 (C=S), 151.78 (C=N), 149.84 (HC=N), 138.95 (Ar), 135.34 (Ar), 129.39 (Ar), 128.96 (Ar), 128.58 (Ar), 126.99 (Ar), 124.08 (Ar), 30.89 (C–H); Anal. Cald. For $C_{16}H_{13}N_5O_2S$: C, 56.63; H, 3.86; N, 20.64; S, 9.45: Found: C, 56.50; H, 3.93; N, 20.70; S, 9.39.

4-(4-Hydroxy-3-methoxylbenzylideneamino)-5-benzyl-2*H*-1,2,4-triazole-3(4*H*)-thione (5d)

Red powder; (75%); R_f; 0.42 (chloroform/methanol, 70:30); m.p 190 ℃; Mol. wt: 340.40; IR (neat, cm^{-1}) ν: 3294.44 (OH), 3183.34 (NH), 3029.87 (sp^2 CH), 2981.17 (sp^3 CH), 1647.20 (HC=N), 1597.42, 1576.55, 1547.78, 1502.39 (Ar–C=C), 1336.17 (-CH bending), 1243.46 (C=S); ^{1}H NMR (CD_3COCD_3-d_6, 300 MHz) δ: 11.28 (b, s, 1H, NH), 8.32 (s, 1H, HC=N), 7.32 (t, 2H, J = 8.0 Hz, Ar–H), 7.08 (t, 1H, J = 8.0 Hz, Ar–H), 7.07 (d, 2H, J = 8.10 Hz, Ar–H), 7.06 (s, 1H, Ar–H), 7.05 (d, 1H, J = 8.02 Hz, Ar–H), 6.75 (d, 1H, J = 8.02 Hz, Ar–H), 4.80 (b, s, 1H, OH), 4.27 (s, 2H, C–H), 3.72 (s, 3H, O–C–H); ^{13}C NMR (CD_3COCD_3-d_6, 75 MHz) δ: 186.30 (C=S), 155.30 (C=N), 151.30 (Ar), 148.30 (Ar), 143.33 (HC=N), 137.53 (Ar), 129.93 (Ar), 128.73 (Ar), 127.73 (Ar), 125.73 (Ar), 122.63 (Ar), 117.63 (Ar), 114.23 (Ar), 56.13 (O–C), 38.63 (C–H); Anal. Cald. For $C_{17}H_{16}N_4O_2S$: C, 59.98; H, 4.74; N, 16.46; S, 9.42: Found: C, 59.92; H, 4.77; N, 16.45; S, 9.42.

5-Benzyl-4-(decylideneamino)-2*H*-1,2,4-triazole-3(4*H*)-thione (5e)

Brown powder; (70%); R_f; 0.57 (chloroform/methanol, 70:30); m.p 145 ℃; Mol. wt: 344.52; IR (neat, cm^{-1}) ν: 3274.13 (NH), 2982.54 (sp^2 CH), 2958.42, 2859.80 (sp^3 CH), 1643.61 (NH Bending), 1629.25 (HC=N), 1595.02, 1549.60, 1508.74 (Ar–C=C), 1445.60 (-CH bending), 1365.58 (-CH bending), 1249.18 (C=S); ^{1}H NMR (CD_3COCD_3-d_6, 300 MHz) δ: 11.28 (b, s, 1H, NH), 7.53 (s, 1H, HC=N), 7.17 (t, 2H, J = 8.0 Hz, Ar–H), 7.10 (t, 1H, J = 8.0 Hz, Ar–H), 7.09 (d, 2H, J = 8.02 Hz, Ar–H), 4.23 (s, 2H, C–H), 2.16 (t, 2H, J = 7.50 Hz, C–H), 1.87 (q, 2H, J = 7.20 Hz, C–H), 1.28–1.49 (m, 12H, C–H), 0.94 (t, 3H, J = 7.20 Hz, C–H); ^{13}C NMR (CD_3COCD_3-d_6, 75 MHz) δ: 186.30 (C=S), 158.33 (C=N), 155.33 (HC=N), 137.53 (Ar),129.13 (Ar), 128.73 (Ar), 125.83 (Ar), 38.63 (C–H), 31.93 (C–H), 29.73 (C–H), 29.53 (C–H), 29.47 (C–H), 29.43 (C–H), 26.73 (C–H), 26.13 (C–H), 22.83 (C–H), 14.23 (C–H); Anal. Cald. For $C_{19}H_{28}N_4S$: C, 66.24; H, 8.19; N, 16.26; S, 9.31: Found: C, 66.15; H, 8.18; N, 16.36; S, 9.31.

4-(3,4,5-Trimethoxybenzylideneamino)-5-benzyl-2*H*-1,2,4-triazole-3(4*H*)-thione (5f)

White powder; (73%); R_f; 0.39 (chloroform/methanol, 70:30); m.p 201 ℃; Mol. wt: 384.46; IR (neat, cm^{-1}) ν: 3280.85 (NH), 3236.14 (sp^2 CH), 2995.58, 2839.31 (sp^3 CH), 1609.74 (HC=N), 1576.32, 1520.40, 1504.89, 1465.71 (Ar–C=C), 1361.42 (-CH bending), 1280.62 (-CH bending), 1248.76 (C=S); ^{1}H NMR (CD_3COCD_3-d_6, 300 MHz) δ: 11.28 (b, s, 1H, NH), 8.13 (s, 1H, HC=N), 7.17 (t, 2H, J = 8.0 Hz, Ar–H),

7.10 (t, 1H, $J=8.0$ Hz, Ar–H), 7.09 (d, 2H, $J=8.02$ Hz, Ar–H), 6.66 (s, 2H, Ar–H), 4.43 (s, 2H, C–H), 3.76 (s, 9H, O–C–H); ^{13}C NMR (CD_3COCD_3-d_6, 75 MHz) δ: 186.93 (C=S), 155.30 (C=N), 150.93 (Ar), 143.30 (HC=N), 141.30 (Ar), 137.30 (Ar), 129.13 (Ar), 128.73 (Ar), 128.13 (Ar), 125.83 (Ar), 106.73 (Ar), 56.65 (O–C), 56.23 (O–C), 38.63 (C–H); Anal. Cald. For $C_{19}H_{20}N_4O_3S$: C, 59.36; H, 5.24; N, 14.57; S, 8.34: Found: C, 59.46; H, 5.20; N, 14.51; S, 8.38.

5-Benzyl-4-(butylideneamino)-2H-1,2,4-triazole-3(4*H*)-thione (5g)

Brown powder; (72%); R_f; 0.53 (chloroform/methanol, 70:30); m.p 260 ℃; Mol. wt: 260.35; IR (neat, cm^{-1}) ν: 3197.12 (NH), 3092.64, 2963.94 (sp^2 CH), 2864.26 (sp^3 CH), 1638.42 (HC=N), 1586.18, 1549.23, 1454.63 (Ar–C=C), 1419.52 (-CH bending), 1376.10 (-CH bending), 1274.30 (C=S); ^{1}H NMR (CD_3COCD_3-d_6, 300 MHz) δ: 11.31 (b, s, 1H, NH), 7.53 (s, 1H, HC=N), 7.17 (t, 2H, $J=8.0$ Hz, Ar–H), 7.10 (t, 1H, $J=8.0$ Hz, Ar–H), 7.09 (d, 2H, $J=8.02$ Hz, Ar–H), 4.36 (s, 2H, C–H), 2.21 (t, 2H, $J=7.50$ Hz, C–H), 1.64 (sixtet, $J=7.50$ Hz, C–H), 0.97 (t, 3H, $J=7.50$ Hz, C–H); ^{13}C NMR (CD_3COCD_3-d_6, 75 MHz) δ: 186.30 (C=S), 158.33 (C=N), 155.30 (HC=N), 137.53 (Ar), 129.13 (Ar), 128.73 (Ar), 125.83 (Ar), 38.63 (C–H), 28.93 (C–H), 19.43 (C–H), 14.02 (C–H); Anal. Cald. For $C_{13}H_{16}N_4S$: C, 59.97; H, 6.19; N, 21.52; S, 12.32: Found: C, 59.80; H, 6.30; N, 21.58; S, 12.32.

In vitro biological evaluation

Biological evaluation was performed through numerous in vitro assays including antioxidant, cytotoxic and α-glucosidase to assess the biological potential of the synthesized derivatives (**3, 5(a–g)).** All the in vitro assays were performed following some standard literature protocols.

DPPH free radical scavenging assay (FRSA)

DPPH (2,2-diphenyl-1-picrylhydrazyl) is a red color free radical having an absorbtion at a wavelength of 517 nm and turns yellow upon its elimination. FRSA of the synthesized derivatives (**3, 5(a–g)**) was assessed from a reported methodology [57]. Ascorbic acid served as a positive control and DMSO served as a negative control. The FRS potential in terms of % inhibition is given in Table 1 and was determined from Eq. (1) provided.

$$\% \text{ Inhibition} = \frac{(\text{Absorbance of the Control} - \text{Absorbance of the Sample})}{\text{Absorbance of the Control}} \times 100$$

Table 1 Structures of the synthesized 5-benzyl-4-(benzylideneamino)-2*H*-1,2,4-triazole-3(4*H*)-thiones derivatives **5(a–g)**

S. No.	Compound	R	S. No.	Compound	R
1	5a	C_2H_5	5	5e	$CH_3(CH_2)_8$
2	5b	4-Cl	6	5f	3,4,5-tri-OCH_3
3	5c	4-NO_2	7	5 g	C_3H_7
4	5d	4-OH, 3-OCH_3	…	…	…

Brine shrimp lethality assay

Brine shrimp lethality assay is a simple, high throughput screening test used to determine the cytotoxicity of the compounds based on their ability to kill a simple zoological organism-brine shrimp (*Artemia salina*). The synthesized derivatives (**3, 5(a–g)**) were tested in a 24-h lethality assay performed in a 96-well plate against Artemia salina (Ocean star, USA) [58]. The eggs of Artemia salina were incubated for a hatching period of 24–48 h under light and warmth (30–32 °C) in simulated seawater (38 g/l supplemented with 6 mg/l dried yeast) in a specially designed two-compartment plastic tray. Using Pasteur pipette, mature phototropic nauplii were harvested and transferred to each well of plate. The corresponding volume of each derivative containing ≤ 1% DMSO in seawater at final concentrations of 200, 100, 50, 25 , and 12.50 µg/ml was transferred to the wells containing seawater and shrimp larvae. The final volume in each well was kept 300 µl. Positive and negative control wells included serial concentrations (50, 25, 12.5, 6.25, and 3.125 ug/ml) of doxorubicin and 1% DMSO in seawater, respectively. After 24-h incubation, live shrimps were counted, and the percentage of deaths was determined. TableCurve 2D v5.01 software was used to calculate median lethal concentration (LC_{50}). The assay was done in triplicate.

Protein kinase inhibition assay

Kinases are an important class of enzymes that phosphorylate their substrate proteins. The assay was performed in triplicates by observing hyphae formation in purified isolates of Streptomyces 85E strain [59]. The bacterial

lawn was allowed to grow by spreading spores (mycelia fragments) of refreshed culture of Streptomyces on sterile plates containing minimal ISP4 medium. About 5 µl of each of the synthesized derivative (20 mg/ml of DMSO) was loaded onto sterile 6 mm filter paper discs. The impregnated paper discs with a final concentration of 100 µg/disc were applied directly on the surface of the plates seeded with Streptomyces 85E. DMSO served as a negative control, and surfactin infused discs served as a positive control. The plates were then incubated at 30 °C for 72 h (time required for hyphae formation in Streptomyces 85E), and the results were interpreted as bald zone of inhibition around samples and controls infused discs.

α-glucosidase inhibition assay

α-Glucosidase is a glucosidase enzyme that is present in the brush border of the small intestine and cleaves $\alpha\,(1\rightarrow4)$ bond of starch. The *α*-glucosidase assay was performed using a literature reported methodology [60]. The assay involves addition of 25 µl of 20 mM substrate solution, 69 µl of 50 mM phosphate buffer, and 5 µl of test sample from 4 mg/ml DMSO stock solution. Subsequently, 1 µl of enzyme solution was added into the designated wells of 96 well plate. The mixture was incubated at 37 °C for half an hour. Following incubation, 100 µl of 0.5 mM sodium bicarbonate solution was added to stop the reaction and absorbance was estimated at 405 nm using microplate reader. Percent enzyme inhibition was calculated using Eq. (1):

$$\%\ \text{Inhibition} = \frac{(\text{Absorbance of the Control} - \text{Absorbance of the Sample})}{\text{Absorbance of the Control}} \times 100$$

Negative control was employed in the assay using the same procedure just by replacing the test derivative with 5 µl DMSO. Acarbose was used as a positive control, and the assay was run in triplicate.

Molecular docking study

Molecular docking (MD) analysis was performed using molecular operating environment (MOE) [61] to explore the binding mode of the screened derivatives **(3, 5(a–g))** against kinases (i.e., *α*-IKK and *β*-IKK) and *α*-glucosidase enzymes. First, the 3D coordinates for the screened derivatives were generated using the MOE-builder module and were protonated, and energy minimized using the default parameters of the MOE (gradient: 0.05, Force Field: MMFF94X). The crystal structure for *α*-IKK and *β*-IKK was retrieved from the protein databank (PDB code; 3BRT & 3BRV). The active site for all the structures was predicted using a site-finder module implemented in MOE due to the complex crystallographic structure unavailability. Subsequently, we observed a hydrophobic cleft (also revealed in the experimental study for kinases), where all the predicted site spheres appeared, and finally, we selected the large size pocket for MD purposes; the following approached already successfully applied as described in our previous study [62] was utilized. Due to the unavailability of the crystallographic structure of the *α*-glucosidase enzyme, we have used the homology model described in our previous study [63] for docking purposes. All the structure was subjected to MOE for preparation.

Further, the protonation was done using default parameters of the structure preparation module of MOE. Next, all the structure was subjected to energy minimization to get minimal energy conformation. Finally, refined structures were used for docking study using the default parameters of MOE; Placement: Triangle Matcher, rescoring 1: London dG, Refinement: Forcefield, Rescoring 2: GBVI/WSA. Before running the docking protocol, a total of five conformations for the ligand were selected. The top-ranked conformations based on docking score (S) and protein–ligand interaction (PLI) profile were selected for analysis.

Statistical analysis

The data obtained from this research work are presented in mean ± SD terms. One-way analysis of variance was carried out to find out variability among groups by Statistix 8.1. The different graphs were obtained using GraphPad Prism 5. Tukey's multiple comparison tests were used to calculate significant differences among groups. The statistical significance was set at $P < 0.05$.

Results and discussion

Synthetic work

The synthesis of 4-amino-5-benzyl-2*H*-1,2,4-triazole-3(4*H*)-thione **(3)** and 5-benzyl-4-(benzylideneamino)-2*H*-1,2,4-triazole-3(4*H*)-thiones **5(a–g)** was performed as depicted clearly in Scheme 1. The first step involves the synthesis of an intermediate 4-amino-5-benzyl-2*H*-1,2,4-triazole-3(4*H*)-thione from phenylacetic acid and thiocarbohydrazide. The synthetic work is performed by fusing phenylacetic acid and thiocarbohydrazide at high temperatures. The reaction completes in a shorter period without any side products. In the second step, the synthesized

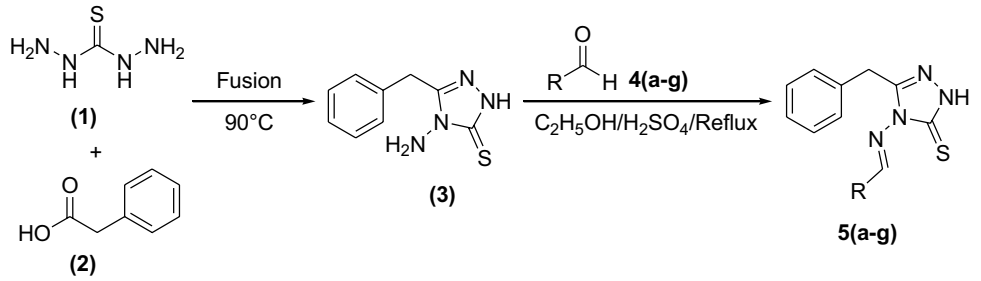

Scheme 1 Synthetic scheme adopted for the synthesis of 5-benzyl-4-(benzylideneamino)-2*H*-1,2,4-triazole-3(4*H*)-thiones **5**(**a–g**)

4-amino-5-benzyl-2*H*-1,2,4-triazole-3(4*H*)-thione was transformed into 5-benzyl-4-(benzylideneamino)-2*H*-1,2,4-triazole-3(4*H*)-thiones **5(a–g)** using substituted aldehydes in dry distilled ethanol. This reaction involves the use of a catalytic amount of concentrated sulfuric acid. Once the synthetic work was performed, the next step involved was to confirm the structures of the synthesized 5-benzyl-4-(benzylideneamino)-2*H*-1,2,4-triazole-3(4*H*)-thiones **5(a–g)** using spectral data (FT-IR, ^{1}H and ^{13}C NMR) and elemental analysis (CHNS).

Spectroscopic characterizations

Structural assignments of the synthesized 4-amino-5-benzyl-2*H*-1,2,4-triazole-3(4*H*)-thione **(3)** and 5-benzyl-4-(benzylideneamino)-2*H*-1,2,4-triazole-3(4*H*)-thiones **5**(**a–g**) were established from elemental (CHNS) and spectroscopic analysis (FT-IR, ^{1}H and ^{13}C NMR). The elemental analysis provided % results for the elements C, H, N and S closely aligned with the structural formula of the synthesized 5-benzyl-4-(benzylideneamino)-2*H*-1,2,4-triazole-3(4*H*)-thiones **5**(**a–g**). FT-IR spectrum of 4-amino-5-benzyl-2*H*-1,2,4-triazole-3(4*H*)-thione **(3)** shows broader absorption bands at 3286.44, 3237.35, 3148.91 cm^{-1} representing NH_2 and NH protons. These NH and NH_2 protons are evident as broader signals from the ^{1}H NMR spectrum at their respective position of 13.54 and 4.02 ppm, respectively. FT-IR spectra of the synthesized 5-benzyl-4-(benzylideneamino)-2*H*-1,2,4-triazole-3(4*H*)-thiones **5**(**a–g**) lack peaks for the NH_2 group protons at 3286.44, 3237.35 cm^{-1}, and sharp singlet is observed for the azomethine (HC=N) linkages in the range of 1651.33–1609.74 cm^{-1}. The azomethine linkages are also evident from ^{1}H NMR spectra of the synthesized 5-benzyl-4-(benzylideneamino)-2*H*-1,2,4-triazole-3(4*H*)-thione **5**(**a–g**) as sharp singlets in the range of 10.81–7.53 ppm. The coupling pattern of the para-substituted phenyl ring protons **(5c)** display double doublets at 8.40 and 8.19 ppm [55].

In vitro biological evaluations

Biological screening of the synthesized 5-benzyl-4-(benzylideneamino)-2*H*-1,2,4-triazole-3(4*H*)-thiones (**3, 5(a–g)**) was performed through various in vitro biological assays like DPPH free radical scavenging (anti-oxidant assay), brine shrimp lethality, protein kinase inhibition (cytotoxicity assay) and α-glucosidase (antidiabetic assay). The in vitro assays were performed by preparing solutions of the synthesized derivatives (**3, 5**(**a–g**)) in DMSO (4 mg/ml, 20 mg/ml) following some well-established standard protocols from the literature. Then serial dilutions of the prepared solutions were performed to prepare their solutions with different concentrations.

DPPH free radical scavenging assay

In vitro DPPH free radical scavenging assay was performed for the synthesized derivatives (**3, 5**(**a–g**)) with reference to the control and was related with the standard antioxidant. DPPH is a stable free radical owing to its delocalized electron that gives an absorption band at 517 nm.

Table 2 DPPH free radical scavenging potential of the screened derivatives (**3**, **5**(**a–g**))

S. No.	DPPH free radical scavenging potential		
	Compound	% scavenging (200 µg/ml)	IC_{50} (µg/ml)
1	3	82.89 ± 0.67^{d}	94.87
2	5a	43.0 ± 0.42^{a}	–-
3	5b	63.28 ± 0.56^{b}	165.32
4	5c	45.27 ± 0.21^{a}	–-
5	5d	75.12 ± 0.74^{c}	132.42
6	5e	84.08 ± 0.27^{de}	74.06
7	5f	42.99 ± 0.63^{a}	–-
8	5 g	88.76 ± 0.77^{e}	61.22

This assay is based on the fact that the DPPH free radicals are being quenched by accepting electrons or hydrogen radicals from the donor antioxidants which augments the antioxidant capability of the screened derivatives. The varied results of the FRSA are presented in terms of their % inhibition as well as IC_{50} (µg/ml) values in Table 2. Accordingly, the antioxidant assay was evaluated initially at 200 µg/ml and the screened derivatives showing significant activity were further screened at lower concentrations (100, 50, 25, and 12.5 ug/ml) in order to determine their IC_{50} values. The highest % free radical inhibition was shown by the derivatives (**5 g), (5e)** and (**3**) with more than 80% of DPPH free radical inhibition. The % DPPH free radical inhibitory potential of the remaining derivatives decreased in the order of **5d > 5b > 5c > 5a > 5f.** In terms of their IC_{50} values, the screened derivatives (**5 g**), (**5e**) and (**3**) showed significant free radical scavenging potential with IC_{50} values of 61.22, 74.06, and 94.87 µg/ml, respectively. Moreover, marked free radical scavenging potential was shown by the derivatives (**5d**) and (**5b**) with IC_{50} values of 132.42 and 165.32 µg/ml, respectively, well above 100.0 µg/ml. However, the remaining derivatives (**5c**) and (**5a**) as well as (**5f**) did not show any prominent radical scavenging potential [57].

Values are represented as mean ± SD of analysis run in triplicate, means with different superscript letters ($^{a-e}$) in a column specify significant difference at $P < 0.05$. IC_{50} values were calculated using TableCurve 2D v4 software.

In vitro cytotoxicity assays

The cytotoxicity profile of the synthesized derivatives (**3, 5**(**a**–**g**)) was assessed from brine shrimp lethality and protein kinase inhibitory assays.

Brine shrimp lethality assay The cytotoxic screening of the synthesized derivatives (**3, 5**(**a**–**g**)) was performed against brine shrimp larvae to reveal their lethality profile. For brine shrimp lethality assay, the initial concentration employed was 200 µg/ml. Among the screened derivatives, those having noteworthy results were further screened at low concentrations (100, 50, 25, 12.5 ug/ml), and their LC_{50} values were determined. Accordingly, the screened derivatives (**5b**), (**3**) and (**5f**) showed significant percent mortality rate at 200 µg/ml with LC_{50} values of 25.88, 32.94, and 34.87 µg/ml, respectively, as shown in Table 3. Their LC_{50} values were found to be well below 50 µg/ml and hence categorized as highly cytotoxic. Similarly, the screened derivatives (**5 g**) and (**5a**) caused moderate to high cytotoxicity at 200 µg/ml with LC_{50} values of 150.37 and 54.45 µg/ml, respectively. These derivatives were considered as moderately cytotoxic in nature (LC_{50} value ≥ 50 but ≤ 200 µg/ml). The remaining derivatives (**5d**), (**5e**) and (**5c**) showed very low mortality rate and were considered as weakly cytotoxic in nature under the experimental conditions [58].

Protein kinase inhibition assay Protein kinase inhibitory potential of the synthesized derivatives (**3, 5**(**a**–**g**)) was determined at an initial concentration of 100 µg/disc using Streptomyces 85E strain. The results of the zones of inhibition are presented in Table 3. Among the screened derivatives, those derivatives showing more than 12-mm bald zone were considered to have noteworthy kinase inhibitory action, and their lower concentrations were tested. Consequently, in comparison with the reference standard surfactin with bald zone of 25.50 ± 1.0 mm, the maximum inhibitory potential was observed for the derivative (**5e**) with clear and bald zones of 10 ± 0.58 and 15 ± 0.58 mm, respectively.

Table 3 The cytotoxicity assays of the screened 5-benzyl-4-(benzylideneamino)-2*H*-1,2,4-triazole-3(4*H*)-thiones (**3**, **5**(**a**–**g**))

S. No.	Compound	Brine shrimp		Protein kinase inhibition		
		% Mortality 200 µg/ml	LC_{50} µg/ml	Diameter at 100 µg/disc		MIC µg/disc
				Clear zone	Bald zone	
1	3	100 ± 5.7^{a}	32.94	8 ± 0.58	14 ± 1.0^{b}	50
2	5a	80 ± 5.7^{b}	54.45	…	…	
3	5b	100 ± 5.7^{a}	25.88	7 ± 0.58	12 ± 0.58^{c}	100
4	5c	10 ± 5.7^{d}	–	…	8 ± 1.0^{d}	…
5	5d	40 ± 5.7^{c}	–	…	9 ± 1.0^{d}	…
6	5e	20 ± 5.7^{d}	–	10 ± 0.58	15 ± 0.58^{b}	50
7	5f	100 ± 5.7^{a}	34.87	…	…	…
8	5 g	60 ± 5.7^{b}	150.37	7 ± 1.0	14 ± 1.0^{b}	50
9	Doxorubicin	100 ± 0.0^{a}	5.65	–	–	–
10	Surfactin	–	–	–	25.50 ± 1.0^{a}	–
11	DMSO	–	–	–	–	–

Similarly, the derivatives **(3)** and **(5 g)** displayed the next higher kinase inhibitory potential with clear and bald zones of 08 ± 0.58 and 14 ± 1.0 mm for the derivative **(3)** and 07 ± 1.0 and 14 ± 1.0 mm for the derivative **(5 g)**, respectively. However, the MIC values obtained for these three derivatives were found to be 50 µg/disc. The remaining derivatives displayed lower kinase inhibitory potential with bald zones much lower than the reference standard surfactin [59].

Values presented are the mean ± SD (n = 3) values analysis run in triplicate. Results of standards are given in respective columns. Means with different superscripts (a–d) represent significantly different values at $p < 0.05$. LC_{50} values were calculated using TableCurve 2D v4 software.

In vitro *α*-glucosidase assay α-glucosidase inhibition assay was employed to determine the antidiabetic potential of the synthesized derivatives (**3, 5**(**a-g**)) at an initial concentration of 100 µg/ml. Results of the α-glucosidase inhibition assay are given in Fig. 2 as mean ± SEM of the % inhibition of α-glucosidase. Among the screened derivatives, (**3**) and (**5e**) showed notable glucosidase inhibitory potential (66.78 and 55.15%). The inhibitory potential was determined in terms of their IC_{50} value. The IC_{50} value was found to be 36.11 µg/ml and 60.33 µg/ml in case of (**3**) and (**5e**)**.** The remaining derivatives were found to be less potent with % α-glucosidase inhibitory potential lower than 50%; hence, there IC_{50} values cannot be determined. However, their inhibitory potential was found to decreasing in the order of **5f > 5d > 5a > 5c > 5b > 5 g** [60].

Molecular docking study

α-IKK and *β*-IKK

The MD results revealed that all the screened derivatives (**3, 5**(**a**–**g**)) showed the best-fit well pattern of binding in the predicted active site for both α- and β-kinase enzyme by site finder module implemented in MOE.

In the case of ***α-IKK***, we have noticed that all the derivatives **(3, 5(a–g))** possess different substituted groups, i.e., electron-donating groups (EDG's) or electron-withdrawing groups (EWG's) as shown in the ribbon representation in Fig. 3a. In the case of the most potent derivatives **(5e and 3),** the highest in vitro activity and several favorable interactions with critical residues which might have a role in the enhancement of the activity of the corresponding enzyme from the MD perspective were observed. The potent derivatives **(5e and 3)** shared similar protein–ligand interaction (PLI) profile, but the only differences found were in their prospective docking score (DS), which was 5.4 for **(5e)** (Fig. 3b) and 4.5 for **(3)** (Fig. 3c). In the case of **(5e),** the R101 participated in arene–cation interaction with the 5-ring, and the Q98 adopted side-chain donor interaction with the sulfur, which is a typical interaction in both compounds.

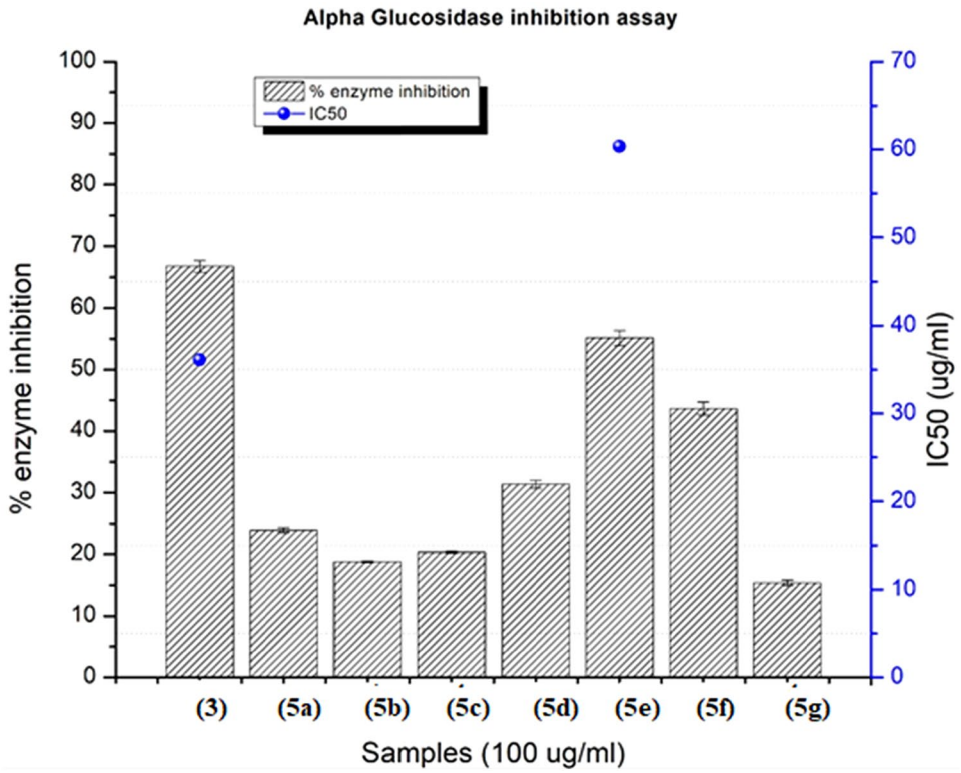

Fig. 2 α-Glucosidase inhibitory potential of the screened derivatives (**3, 5**(**a–g**)): Results are expressed as mean ± SD of percent inhibition of the α-glucosidase enzyme. Acarbose was used as a positive control, and its IC_{50} value was found to be 4.2 µg/ml. DMSO was used as a negative control with enzyme inhibition noted. IC_{50} values were calculated using TableCurve 2D v4 software

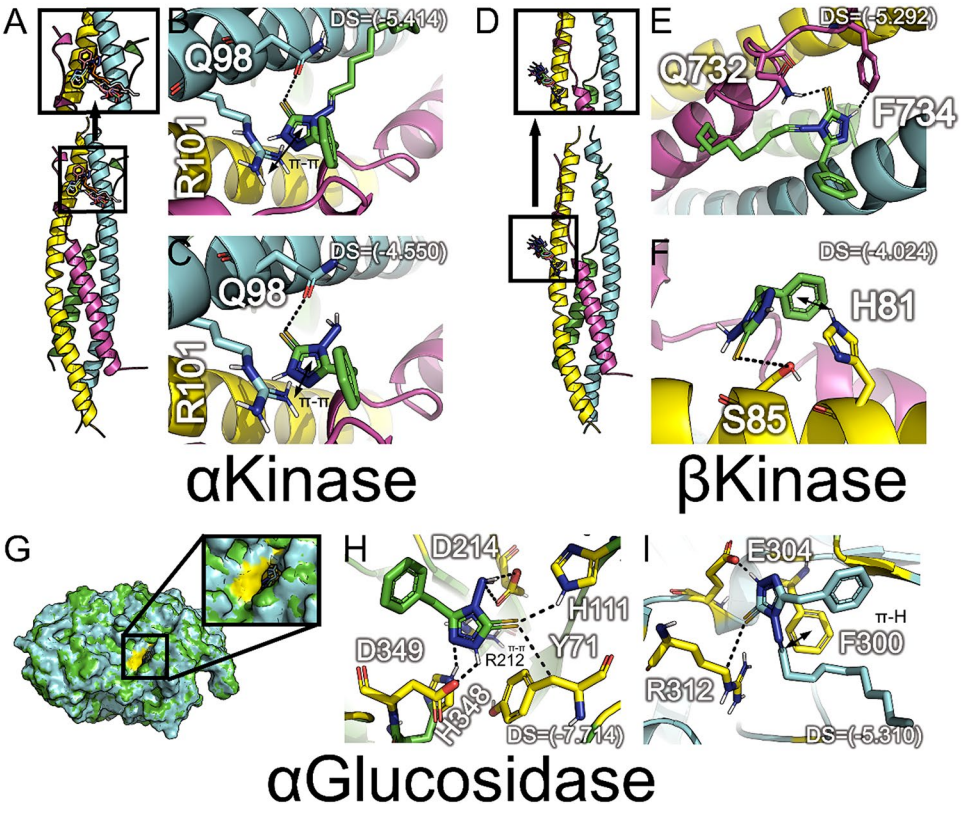

Fig. 3 The protein–ligand interaction (PLI) profiles against kinase (α-IKK and β-IKK) and α-glucosidase enzyme. (**a**) indicates the α-IKK enzyme surface, (**b**, **c**) Represent the PLI profile for the derivatives **(5e and 3).** (**d**) shows the surface of the β-IKK enzyme. (**e**, **f**) Represent the PLI profile for the derivatives **(5e)** and **(3).** (**g**) shows the surface representation of the α-glucosidase enzyme. (**h**, **i**) Represent the PLI profile for the derivatives **(3)** and **(5e).** Double-sided arrows represent the arene–arene interaction

In the case of ***β-IKK***, the potent derivatives **(5e and 3)** shared different PLI profile with key residues, but the only similarity found was, in their interacting mode; the sulfur (S) atom of the 4-methyl-2*H*-1,2,4-triazole-3(4*H*)-thione moiety participated in interaction with different residues (Fig. 3d–f). For example, the experimental results indicate the importance of hydrophobic residue F734, which plays an essential role in interaction with other proteins. In our case, we observed that the derivative **(5e)** adopted hydrogen bond interaction with the 5-ring structure of the ligand. Also, we observed that the nearby residues to this critical residue F734 also participated in the interaction. Due to the triggering of these important residues, it might be allosterically raised the inhibitory potential of this compound. The nearby residue at a distance ~ 2-3 angstrom includes the polar uncharged side-chain residue, i.e., Q732. Both the residues shared a similar interaction, as the only difference found in their side-chain moiety. Generally, the excellent potential of the **(5e)** against the beta-kinase might be due to the triggering potential of the critical important residue F734, which might trigger other residues to participate in the interaction. Also, the binding pose of 5e is similar to a cage-like structure, where both the hydrophobic and polar uncharged side-chain residues rescue the compound from dissociation.

α-glucosidase

The molecular docking results for both the derivatives **(3 and 5e)** against the α-glucosidase enzymes revealed that the derivative **(3)** showed the best inhibitory potential based on the PLI profile and the docking score. The active site was mostly occupied by polar and acidic residues and some hydrophobic residues supporting the bridge for maintaining the interaction (Fig. 3g). In the case of the potent derivatives **(3),** the PLI profile revealed that the derivative mostly adopted favorable interactions with polar (H111, Y71, H348) and acidic (D349 and D214) residues, and only one essential residue (R212) was found, as shown in Fig. 3h. Both the derivative shared a typical interaction moiety (sulfur), as was observed in kinase activity. In the case of the second most potent derivative **(5e),** we have noticed that only one acidic (E304) and basic (R312) and one additional hydrophobic (F300) residue adopted interaction with the derivative (Fig. 3i). The derivative **(3)** high potency might be due to the attached EDG (NH2), which has a substantial activation over others.

Conclusions

This study reports the synthesis and characterization of the 5-benzyl-4-(benzylideneamino)-2*H*-1,2,4-triazole-3(4*H*)-thiones (**3, 5**(**a**–**g**)). The synthesized derivatives were screened in various in vitro assays. As evident from the results, some of the screened derivative displayed dose-dependent response in the tested in vitro assays. The derivatives (**5 h**), (**5f**), and (**5a**) showed significant free radical scavenging potential with IC_{50} values of 61.22, 74.06, and 94.87 µg/ml, respectively. The derivatives (**5c**), (**5a**), and (**5 g**) showed significant percent mortality at 200 µg/ml with LC_{50} values of 25.88, 32.94, and 24.87 µg/ml, respectively. In case of protein kinase inhibitory assay, the maximum inhibitory potential was observed in case of (**5f**) and (**5a**) with MIC that was observed to be 50 µg/disc in both cases. Moreover, the derivatives (**5a**) and (**5f**) showed notable enzyme inhibitory action with IC_{50} values of 36.11and 60.33 µg/ml, respectively. Thus, based on the results, it can be concluded that the screened 4-amino-5-benzyl-2*H*-1,2,4-triazole-3(4*H*)-thione and their 5-benzyl-4-(benzylideneamino)-2*H*-1,2,4-triazole-3(4*H*)-thiones possess better inhibitory potential for the α-glucosidase and Kinases.

Acknowledgements The author Mr. Hamid Aziz gratefully acknowledges the financial support of the Higher Education Commission (HEC), Pakistan, by awarding indigenous scholarship phase-II for Ph.D. studies.

References

1. Y. Murti, R. Agnihotri, D. Pathak, Am. J. Chem. **1**(2), 42–46 (2011)
2. K. Carter, R. Miller, J. Hedrick, Polymer **34**(4), 843–848 (1993)
3. N.S. Vatmurge, B.G. Hazra, V.S. Pore, F. Shirazi, P.S. Chavan, M.V. Deshpande, Bioorg. Med. Chem. Lett. **18**(6), 2043–2047 (2008)
4. L. Navidpour, H. Shafaroodi, K. Abdi, M. Amini, M.H. Ghahremani, A.R. Dehpour, A. Shafiee, Bioorg. Med. Chem. **14**(8), 2507–2517 (2006)
5. Z.H. Chohan, S.H. Sumrra, M.H. Youssoufi, T.B. Hadda, Eur. J. Med. Chem. **45**(7), 2739–2747 (2010)
6. B. Blank, D.M. Nichols, P.D. Vaidya, J. Med. Chem. **15**(6), 694–696 (1972)
7. T.O. Okuno, S. Oikawa, T. Goto, K. Sawai, H. Shirahama, T. Matsumoto, Agirc. Biol. Chem. **50**(4), 997–1001 (1986)
8. E. Bokor, T. Docsa, P. Gergely, L. Somsak, A.C.S. Med, Chem. Lett. **4**(7), 612–615 (2013)
9. C. Ainsworth, N.R. Easton, M. Livezey, D. Morrison, W. Gibson, J. Med. Chem. **5**(2), 383–389 (1962)
10. C. Radhika, A. Venkatesham, M. Sarangapani, Med. Chem. Res. **21**(11), 3509–3513 (2012)
11. N. Boechat, L. Pinheiro, O.A. Santos-Filho, I.C. Silva, Molecules **16**(9), 8083–8097 (2011)
12. D.J. Williamson, R.G. Hill, S.L. Shepheard, R.J. Hargreaves, Br. J. Pharmacol. **133**(7), 1029–1034 (2001)
13. S.G. Khanage, A. Raju, P.B. Mohite, R.B. Pandhare, Adv. Pharm. Bull. **3**(1), 13–18 (2013)
14. J.P. Malerich, J.S. Lam, B. Hart, R.M. Fine, B. Klebansky, M.J. Tanga, A. D'Andrea, Bioorg. Med. Chem. Lett. **20**(24), 7454–7457 (2010)
15. A.K. Jordao, P.P. Afonso, V.F. Ferreira, M.C. De Souza, M.C. Almeida, C.O. Beltrame, D.P. Paiva, S.M. Wardell, J.L. Wardell, E.R. Tiekink, Eur. J. Med. Chem. **44**(9), 3777–3783 (2009)
16. M. Maletic, A. Leeman, M. Szymonifka, S.S. Mundt, H.J. Zokian, K. Shah, J. Dragovic, K. Lyons, R. Thieringer, A.H. Vosatka, Bioorg. Med. Chem. Lett. **21**(8), 2568–2572 (2011)
17. N. Di Mola, E. Bellasio, Farmaco-Ed. Sci. **40**(7), 517–533 (1985)
18. L.V. Rodriguez, J.P. Dedet, V. Paredtes, C. Mendoza, F. Cardenas, Mem. I Oswaldo. Cruz. **90**(4), 525–528 (1995)
19. A.K. Jordao, V.F. Ferreira, E.S. Lima, M.C. De Souza, E.C. Carlos, H.C. Castro, R.B. Geraldo, C.R. Rodrigues, M.C. Almeida, A.C. Cunha, Bioorg. Med. Chem. **17**(10), 3713–3719 (2009)
20. V. Calderone, I. Giorgi, O. Livi, E. Martinotti, E. Mantuano, A. Martelli, A. Nardi, Eur. J. Med. Chem. **40**(6), 521–528 (2005)
21. K. Ilango, P. Valentina, Der. Pharm. Chem. **2**(2), 16–22 (2010)
22. J. He, L. Feng, J. Li, R. Tao, F. Wang, X. Liao, Q. Sun, Q. Long, Y. Ren, J. Wan, Bioorg. Med. Chem. **20**(5), 1665–1670 (2012)
23. K. Oh, K. Yamada, T. Asami, Y. Yoshizawa, Bioorg. Med. Chem. Lett. **22**(4), 1625–1628 (2012)
24. B.F. Abdel-Wahab, S.F. Mohamed, A.E.G.E. Amr, M.M. Abdalla, Monatshefte für Chemie-Chem. Mon. **139**(9), 1083–1090 (2008)
25. A.A. Siddiqui, R. Mishra, M. Shaharyar, A. Husain, M. Rashid, P. Pal, Bioorg. Med. Chem. Lett. **21**(3), 1023–1026 (2011)
26. A.M. Iqbal, A.Y. Khan, M.B. Kalashetti, N.S. Belavagi, Y.D. Gong, I.A.M. Khazi, Eur. J. Med. Chem. **53**, 308–315 (2012)
27. T. Akhtar, S. Hameed, N.A. Al-Masoudi, K.M. Khan, Heteroatom. Chem. Int. J. Main Group Elem. **18**(3), 316–322 (2007)
28. S.N. Pandeya, D. Sriram, G. Nath, E. De Clercq, Arzneimittelforschung **50**(1), 55–59 (2000)
29. B.B. Sokmen, N. Gumrukcuoglu, S. Ugras, H. Sahin, Y. Sagkal, H.I. Ugras, Appl. Biochem. Biotech. **175**(2), 705–714 (2015)
30. K.M. Khan, S. Siddiqui, M. Saleem, M. Taha, S.M. Saad, S. Perveen, M.I. Choudhary, Bioorg. Med. Chem. **22**(22), 6509–6514 (2014)
31. D.D. Erol, U. Çaliş, R. Demirdamar, N. Yuluğ, M. Ertan, J. Pharm. Sci. **84**(4), 462–465 (1995)
32. S. Chen, Y.C. Kao, C.A. Laughton, J. Steroid Biochem. Mol. Biol. **61**(3–6), 107–115 (1997)
33. B. Baumann, I.R. Baxendale, S.V. Ley, N. Nikbin, Beilstein. J. Org. Chem. **7**(1), 442–495 (2011)
34. N.H.N. Moorthy, U.B. Vittal, C. Karthikeyan, V. Thangapandian, A.P. Venkadachallam, P. Trivedi, Arab. J. Chem. **10**, S3239–S3244 (2017)
35. K.S. Solanki, G. Pal, H. Haider, M.K. Singh, J.S. Kothari, V.K. Agarwal, U.S. Patent Application 11/992,708 (2009).
36. P.C. Ray, M. Bandari, M. Qadeeruddin, S.R. Gorantla, U.S. Patent Application 12/093,683 (2009).
37. E. Richmond, I.U. Khan, J. Moran, Chem. A. Eur. J. **22**(35), 12274–12277 (2016)
38. A. Prakash, D. Adhikari, Int. J. Chem. Tech. Res. **3**(4), 1891–1896 (2011)
39. G.B. Bagihalli, P.S. Badami, S.A. Patil, J. Enz. Inhibit. Med. Chem. **24**(2), 381–394 (2009)
40. A. Iqbal, H. Siddiqui, C. Ashraf, M. Ahmad, G. Weaver, Molecules **12**(2), 245–254 (2007)
41. A.K. Sadana, Y. Mirza, K.R. Aneja, O.M. Prakash, Eur. J. Med. Chem. **38**(5), 533–536 (2003)
42. A. Hameed, M. Al-Rashida, M. Uroos, S.A. Ali, K.M. Khan (2017) Expert opinion on therapeutic patents **27**(1), 63–79
43. M. Hanif, Z.H. Chohan, Spectrochim. Acta Part A Mol. Biomol. Spectrosc. **104**, 468–476 (2013)

44. I.U. Khan, R. Bibi, A. Hassan, Curr. Org. Chem. **22**(25), 2460–2486 (2018)
45. M. Maneiro, M.R. Bermejo, M.I. Fernandez, E. Gómez-Fórneas, A.M. González-Noya, A.M. Tyryshkin, New J. Chem. **27**(4), 727–733 (2003)
46. A. Murugkar, R. Bendre, A. Kumbhar, S. Padhye, R. Pritchard, C.A. McAuliffe, Indian J. Sec. A Inorg. Bio-Inorg. Phys. Theoret. Analyt. Chem. **38**(10), 977–980 (1999)
47. T. Joseph, D.P. Sawant, C.S. Gopinath, S.B. Halligudi, J. Mol. Catal. A Chem. **184**(1–2), 289–299 (2002)
48. A.R. Fakhari, A.R. Khorrami, H. Naeimi, Talanta **66**(4), 813–817 (2005)
49. R.J. Young, G.W. Cooper, Reproduction **69**(1), 1–10 (1983)
50. Z.H. Chohan, M. Praveen, A. Ghaffaf, Synth. React. Inorg. Metal-org. Chem. **28**(10), 1673–1687 (1998)
51. A.F. Alghamdi, N. Rezki, J. Taibah Univ. Sci. **11**(5), 759–767 (2017)
52. J.Y. Jin, L.X. Zhang, A.J. Zhang, X.X. Lei, J.H. Zhu, Molecules **12**(8), 1596–1605 (2007)
53. G.B. Bagihalli, P.G. Avaji, S.A. Patil, P.S. Badami, Eur. J. Med. Chem. **43**(12), 2639–2649 (2008)
54. P. Anand, V.M. Patil, V.K.M. Sharma, R.L. Khosa, N. Masand, Int. J. Drug Des. Disc. **3**, 851–868 (2012)
55. A.M. Isloor, B. Kalluraya, P. Shetty, Eur. J. Med. Chem. **44**(9), 3784–3787 (2009)
56. R.R. Pillai, K. Karrouchi, S. Fettach, S. Armaković, S.J. Armaković, Y. Brik, J. Taoufik, S. Radi, M.E.A. Faouzi, M.H. Ansar, J. Mol. Struct. **1177**, 47–54 (2019)
57. M. Umamaheswari, T.K. Chatterjee, Afr. J. Trad. Comp. Altern. Med. **5**(1), 61–73 (2008)
58. I. Ul-Haq, N. Ullah, G. Bibi, S. Kanwal, M.S. Ahmad, B. Mirza, Iran. J. Pharm. Res. **11**(1), 241–249 (2012)
59. G. Yao, F.M. Sebisubi, L.Y.C. Voo, C.C. Ho, G.T. Tan, L.C. Chang, J. Braz. Chem. Soc. **22**(6), 1125–1129 (2011)
60. S.S. Nair, V. Kavrekar, A. Mishra, Eur. J. Exp. Biol. **3**(1), 128–132 (2013)
61. Molecular Operating Environment (MOE), 2016.08; Chemical Computing Group Inc.
62. 1010 Sherbrooke St. West, Suite #910, Montreal, QC, Canada, H3A 2R7, 2016.
63. F. Jabeen, S.S. Panda, T.P. Kondratyuk, E.H. Park, J.M. Pezzuto, C.D. Hall, A.R. Katritzky, Bioorg. Med. Chem. Lett. **25**(15), 2980–2984 (2015)